INVITED FEATURE PAPER

Transparent electrodes made from carbon nanotube polyelectrolytes and application to acidic environments

Amélie Catheline[b)]
CNRS, Centre de Recherche Paul Pascal (CRPP), UPR 8641, F-33600, Pessac, France; and Université de Bordeaux, CRPP, UPR 8641, F-33600, Pessac, France

Francesco Paolucci and Giovanni Valenti
Dipartimento di Chimica, Università di Bologna, Via Selmi 2, I-40126, Bologna, Italy

Philippe Poulin and Alain Pénicaud[a)]
CNRS, Centre de Recherche Paul Pascal (CRPP), UPR 8641, F-33600, Pessac, France, Université de Bordeaux, CRPP, UPR 8641, F-33600, Pessac, France

(Received 23 February 2015; accepted 27 May 2015)

Carbon nanotube (CNT)-based transparent conducting films (TCFs) have been prepared by filtration of (i) surfactant-based aqueous dispersions and (ii) organic solutions obtained by reductive dissolution of an alkali metal salt of polyelectrolyte nanotubes. Starting from the same source of nanotubes, it is shown that films obtained by the reductive dissolution route present up to one order of magnitude better conductivity for the same transmittance. Light scattering experiments show that the average CNT length is much larger for the reductive dissolution-based organic solutions than for the sonication aided aqueous dispersions. Values of surface resistivity of 200 ohm per square have been obtained for 80% transmittance. Additionally, it is shown that the CNT-based TCFs are undistinguishable from indium tin oxide (ITO) as electrodes in regular environments, whereas they perform efficiently in acidic environments where ITO fails.

I. INTRODUCTION

Carbon nanotubes (CNTs) are promising for applications in different fields, such as electronics,[1–3] fibers,[4–6] sensors,[7,8] and composites.[9,10] In particular, CNTs are considered as one of the most convincing alternative to inorganic oxides for future transparent electrodes. As CNTs are practically insoluble in all solvents, different methods have been developed, using sonication or high shear mixing, to disperse CNTs in water or in organic solvents. CNT aqueous dispersions can be obtained using surfactants and sonication.[11] Nevertheless, these methods are known to damage CNTs, creating defects on the walls of nanotubes[12] and shortening them.[13,14] An alternative method known as reductive dissolution has been developed[15–19] in which CNTs are reduced by potassium naphthalide in Tetrahydrofuran (THF).[20] A negatively charged CNT salt is obtained, which is spontaneously soluble in polar aprotic solvents, such as Dimethyl sulfoxide (DMSO). No sonication is used. It has been shown that the reductive dissolution individualizes nanotubes without damaging them.[21,22] Here we show that transparent conducting films (TCFs) prepared from CNT solutions obtained by reductive dissolution have far better performances than films prepared from aqueous, sonication-aided dispersions. The study is focused on understanding the effects of the reductive dissolution on film electrical performances and on highlighting the key parameters to control these performances. Nanotube length appears to be a key parameter to tune the sheet resistivity of the films. Moreover, it has been shown that indium tin oxide (ITO) can be damaged under acidic conditions.[23] In this article, we show that the electroactivity of CNT films, in addition to their better chemical resistance to acids, allows their use in applications where ITO is unsuitable.

Among different alternative materials,[24] such as graphene[25] and metal electrodes,[26] CNTs are a promising material for the replacement of ITO used in current electronic devices.[27,28] Indeed, ITO has some limitations, such as its brittleness, high cost, and limited supply. New materials with comparable performances are actively sought after. Those materials should ideally exhibit a transmittance higher than 80% and a surface resistivity of 10 Ω/sq.[29] TCFs are one of the possible applications for CNTs as it was shown first by Rinzler et al.[3] CNT thin films can be prepared by different techniques, such as by filtration technique. This method has the advantage of being easily performed and to

Contributing Editor: Mauricio Terrones
[a)]Address all correspondence to this author.
e-mail: penicaud@crpp-bordeaux.cnrs.fr
[b)]New address: Linde Nanomaterials, 1970 Diamond St., San Marcos 92078, CA, USA
This paper has been selected as an Invited Feature Paper.
DOI: 10.1557/jmr.2015.166

 © Materials Research Society 2015

https://doi.org/10.1557/jmr.2015.166 Published online by Cambridge University Press

produce homogeneous network of randomly distributed CNTs. In 2004, Rinzler et al. produced CNT films having a surface resistivity of 30 Ω/sq for 90% transmittance using laser ablation single-walled carbon nanotubes (SWCNTs).[3] Grüner et al. developed a similar method in 2006.[30] In their study, CNT network was transferred by stamping CNTs from filtration membrane on flexible substrates. These CNT films showed a surface resistivity of 120 Ω/sq for 70–80% of transmittance. Pasquali et al. worked on a draw–roll method and obtained CNT films with a surface resistivity of 600 Ω/sq for 90% of transmittance.[31] This method is one of the most promising methods for future scale-up.[32] Other techniques, such as dip coating, spray coating, electrodeposition, or chemical vapor deposition (CVD), have been studied and display interesting features in terms of achieved performances and scalability.[32–34] In particular, using very long nanotubes, Pasquali et al. have obtained films by dip coating that exhibit a 100 Ω/sq resistivity for 90% transmittance.[35]

For clarity, in this article, we call rd-CNTs, CNTs processed by reductive dissolution to prepare the solutions and then the films, whereas the term ad-CNTs are used to describe CNT aqueous dispersions. Using routinely available CNTs from commercial source (MWCNTs from Arkema, FWCNTs (Elicarb™) from Thomas Swan and SWCNTs (CoMoCAT™) from SWeNT), we show that the reductive dissolution avoids cutting the tubes and allows to obtain better performing TCFs, with surface resistance as low as 200 Ω/sq at 80% transmittance reachable for CoMoCAT SWCNTs.

II. TCFs: RESULTS

The so-called membrane filtration method allows the thickness of CNT films to be controlled by varying the volume of filtered solution. As shown in the scanning electron micrograph of Fig. 1, CNT networks are homogeneous. Moreover, measurements by x-ray photoelectron spectroscopy of film surface show that the rinsing process is efficient to obtain clean CNTs, indeed, neither potassium nor surfactant was found on the surface. Atomic force microscopy (AFM) measurements have been performed to characterize the thickness of the films by measuring the depth of a straight scratch made into them [see inset to Fig. 1(a)]. Varying the quantity of filtered solution, the thickness and, therefore, the transmittance of the CNT films can accurately be controlled. Using multiwalled carbon nanotubes (MWCNTs), film thickness can be tuned between 60 and 130 nm for a transmittance between 85 and 60%. Thickness of few-walled carbon nanotubes (FWCNTs) films was found to vary between 30 and 60 nm for a transmittance from 80 to 60%. The difference from MWCNTs suggests that FWCNTs are more densely packed for the same transmittance.

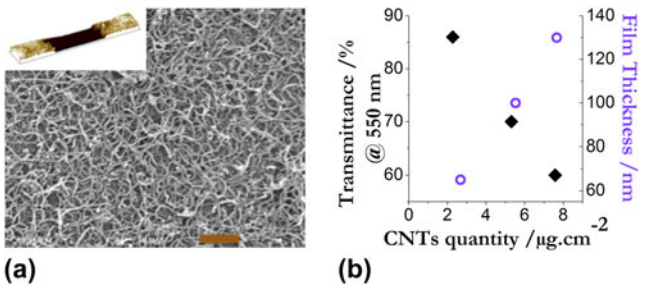


FIG. 1. (a) SEM picture of a MWCNT film. Scale bar is 0.5 micrometer. Inset: AFM image of a scratch made to measure thickness. The actual thickness of this film is 40 nm while the width of the scratch is 20 micrometer. (b) Transmittance and thickness of MWCNT films versus CNT quantity.

Electrical performances of CNT TCFs have been then investigated. Film transmittance versus the surface resistivity is plotted in Fig. 2. Influence of the reductive dissolution route on film performances can be compared to that of the aqueous dispersion method, for MWCNTs and FWCNTs. Considering FWCNT films, surface resistivity is much lower using the solvent method than the aqueous method. At 80% of transmittance, the surface resistivity is about 2500 Ω/sq for films made with rd-FWCNTs, which is an order of magnitude lower than the surface resistivity (about 20,000 Ω/sq) of ad-FWCNT films. A similar result is obtained for MWCNT films, rd-MWCNT films have a surface resistivity of 5000 Ω/sq at 80% of transmittance compared to a surface resistivity of about 100,000 Ω/sq at the same transmittance for ad-MWCNT films. Moreover, we can observe that electrical performances of films depend on the type of CNTs. As shown in Fig. 2, using the same solution preparation, FWCNT films have better electrical performances than MWCNT films at the same transmittance. As sonication is known to shorten CNTs,[14,36] CNT length was investigated and compared for both solution and dispersion methods. CNT length can be measured by dynamic light scattering (DLS) using a method detailed in the literature.[14,36,37] Results show that ad-CNTs are shorter than rd-CNTs. rd-FWCNTs are 1.6 ± 0.1 µm long in organic ink compared to 500 ± 50 nm for ad-FWCNTs in aqueous inks. rd-MWCNTs are 1.7 ± 0.1 µm long in organic inks. They are much shorter in aqueous dispersions, with a length of 320 ± 50 nm. These results show that the reductive dissolution is efficient at maintaining long CNTs in liquids opening thereby an important route to improve the properties of CNT films. We stress that no sonication was used in the above experiments for nanotubes treated by reductive dissolution. This is why their length is greater than that of nanotubes dispersed in water. This holds for all types of CNTs: MWCNTs, FWCNTs and SWCNTs. Effect of length and relation with electrical performances of CNT films is discussed below, thanks to the study of SWCNT films. These films

https://doi.org/10.1557/jmr.2015.166 Published online by Cambridge University Press

were prepared as described above with different batches of CNTs. A first batch of CoMoCAT CG200 CNTs has been used to prepare three solutions (from number 1 to 3) by the solvent method and one aqueous dispersion.

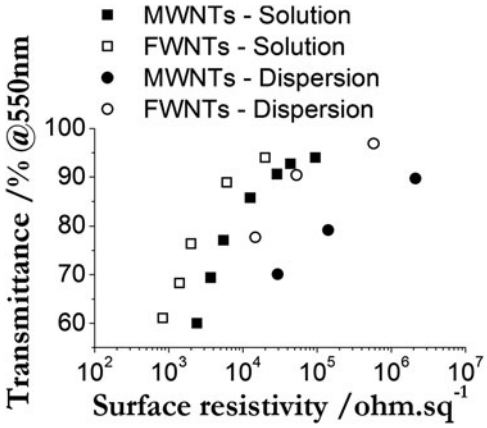


FIG. 2. Transmittance of FWCNT and MWCNT films versus their surface resistivity.

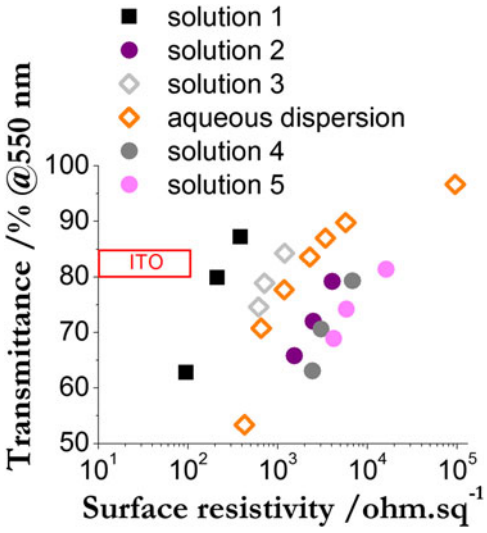


FIG. 3. Transmittance of CNT films versus their surface resistivity. The results are represented in three groups according to the CNT length. Squares correspond to the longest CNTs, about 3.1 μm long. Rhombs correspond to an intermediate length, about 2.2 μm long, and circles represent the shortest CNTs, about 1.5 μm long.

For each solution, 64 mg of raw CNTs were used to prepare a CNT potassium salt that was then dissolved to form ca 8 mL of solution. In spite of originating from the same batch, the resultant solutions have been observed to differ because of the heterogeneity of the raw powder. As seen latter, the variability in the raw powder allowed solutions with nanotubes of different lengths to be investigated. The CNTs in solutions differ in their average length by almost a factor 2. A second batch of CoMoCAT CG200 has been used to prepare solution 4 and a batch of CoMoCAT CG100 to prepare solution 5—both by solvent method. All these inks were done to investigate the reproducibility of electrical performances of SWCNT films. First, using rd-SWCNT solution, good conductive films are obtained. The best films, made with solution 1, have a surface resistivity of 210 Ω/sq at 80% transmittance, which approach ITO performances by roughly one order of magnitude. Nevertheless, Fig. 3 clearly shows that a wide range of surface resistivity is obtained using the same kind of SWCNTs, from 210 to 10,000 Ω/sq at 80%, fact that we ascribe to the heterogeneity of the CNT batch use and the different average CNT lengths in each solution. Following the results obtained for MWCNT and FWCNT solutions and films, DLS measurements have been performed to measure CNT average length. The obtained results are shown in Table I. A link between CNT length and electrical performances of films can clearly be seen. The most conductive films (R_{sq} = 210 Ω/sq, T = 80%) have been prepared with the longest CNTs with a length of about 3.1 μm. The shorter the CNTs, the more resistive are the CNT films. As shown in Fig. 3, results can be separated in three groups: the most conductive films (represented by squares), the most resistive ones (represented by circles), and the intermediate ones (represented by rhombs). As has been amply documented in the literature,[38,39] doping could further improve conductivity of the films but has not been attempted here.

III. TCFs: DISCUSSION

Results show that the surface resistivity of the CNT films depends strongly on the CNT length [Fig. 4].

TABLE I. CNT length measured by DLS for the different inks.

CNT length/nm		rd-CNT ink	ad-CNT ink	
FWCNTs		1600 ± 100	500 ± 50	...
MWCNTs		1700 ± 100	320 ± 50	...
SWCNTs	N°1	3150 ± 300	/	Batch 1 – CoMoCAT CG200
	N°2	1400 ± 100	/	
	N°3	2250 ± 200	/	
	Dispersion	/	2150 ± 200	
	N°4	1550 ± 100	/	Batch 2 – CoMoCAT CG200
	N°5	1500 ± 100	/	CoMoCAT CG100

https://doi.org/10.1557/jmr.2015.166 Published online by Cambridge University Press

This dependency suggests that the conductivity is limited by the contact resistance of the nanotube junctions, as observed in several other nanotube-based composites and transparent electrodes.[33,40–42] Indeed, when the nanotubes are sufficiently long, their resistance exceeds the resistance of a contact. In this regime, the conductivity is not anymore expected to depend on the length of the nanotubes.[43] The conductivity is just expected to depend on the density of nanotubes present in the films. By contrast when nanotubes are short, the conductivity can become length dependent. In particular, close to the percolation threshold, it has been shown that the conductivity is expected to scale as $\sim L^{2.5}$.[43] Note that this is an upper bound only valid close to percolation. At greater concentrations, lower exponents can be expected. In this regime, one has to consider the density of contacts. But the latter is still independent on the nanotube length as long as the volume fraction is kept constant.[44] In brief, depending on the CNT concentration and length, variations of conductivity are expected to vary between scaling laws with exponents from 0 to 2.5.[43] Our experiments are in disagreement with such expectations. They are also in disagreement with previous studies in which the nanotubes were sorted by centrifugation instead of being sorted by length using the sonication method to shorten them.[45] If the data would be fitted by a scaling law, the conductivity would approximately scale as $\sim L^4$ [Fig. 4]. This large variation indicates that the conductivity is limited by the contact resistance between nanotubes, meaning that the nanotubes are not yet long enough so that the film conductivity becomes independent on the nanotube length. But geometrical effects alone cannot explain the present results as the data are outside the range defined by the limiting cases of near percolated networks and constant conductivity.

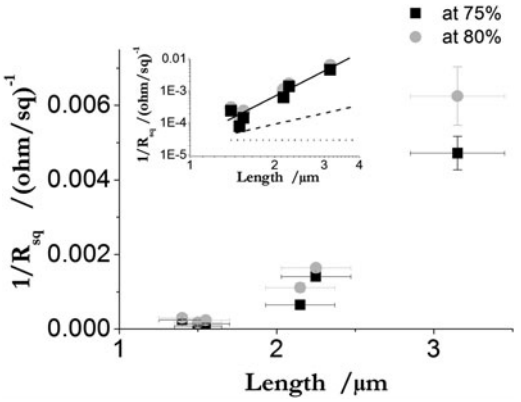


FIG. 4. TCF Conductivity versus CNT length for two sets of TCF transmittance, the inset shows on a log–log scale the experimental data, experimental trend in L^4 (black line), theoretical behaviors for constant conductivity in L^0 (dotted line), and for length dependent conductivity in $L^{2.5}$ (dashed line).

Other effects have, therefore, to be considered. The main deviations from the simplest expectations detailed above are likely due to intrinsic features of the nanotubes. In particular, the density of structural defects is expected to strongly alter the conductivity of the films. Indeed, defects play an important role on the conductivity, since they alter the π conjugation of the nanotubes. The presence of defects has been confirmed by Raman experiments. As shown in Fig. 5, the ratio I_D/I_G increases with the sheet resistance of the TCFs, confirming that the most conductive films are obtained with the less defective nanotubes. Even a slight degradation of the CNT structure can result in a substantial decrease of the conductivity and can likely explain substantial deviations from the length dependence expected for random networks of homogeneous CNTs.

IV. ELECTROACTIVITY OF CNT FILMS

In this section, CNT films are studied as a substitute to ITO electrodes in electrochemical applications. Several studies have already shown that CNTs are electroactive and can be used as electrochemical sensors, for example, to detect insulin,[46] ammonia gas,[47] or traces of heavy metals.[48] CNT catalytic activity has also been studied in dye-sensitized solar cell.[49–52] ITO, on the other

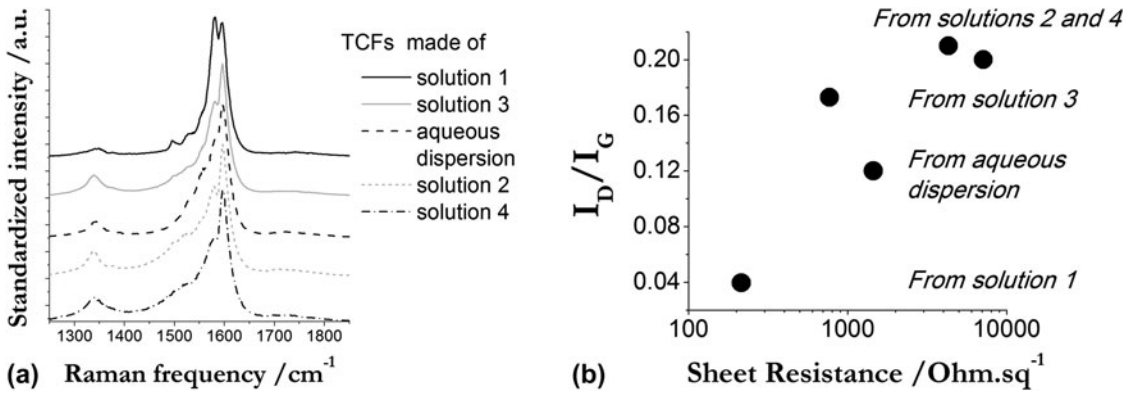


FIG. 5. (a) Raman spectra of the different TCFs and (b) I_D/I_G ratio versus sheet resistance for the TCFs.

https://doi.org/10.1557/jmr.2015.166 Published online by Cambridge University Press

hand, is widely used as electrode material under mild conditions, in particular in organic media,[53] while it is known to be unsuitable under more extreme conditions, as for instance in aqueous solutions, at low pH and negative potentials where it rapidly undergoes an irreversible degradation with a severe loss of conductivity, transparency, and electroactivity.[35,54] Thus, a comparison of CNT films and ITO as electrode materials has been performed at low pH, using a standard redox couple $\left[Fe(CN)_6^{3-}/Fe(CN)_6^{4-}\right]$ to study their electroactivity. Results showed that CNT films can be used in acidic media where ITO is damaged.

rd-CNT films made with SWCNT from both SWeNT (CoMoCAT) and CCNI origin were used to prepare the electrodes, and Fig. 6 shows cyclic voltammograms of potassium ferrocyanide measured with two different CNT films. The high symmetry of the cyclic voltammetry (CV) curves along with the linear dependence of the peak currents on $\nu^{1/2}$ and the invariance of peak potentials with the scan rate (not shown) highlight the expected Nernstian behavior of such a redox couple on the CNT electrodes. Such electrodes are, therefore, virtually indistinguishable from ITO, whose behavior is also shown for comparison in Fig. 6.

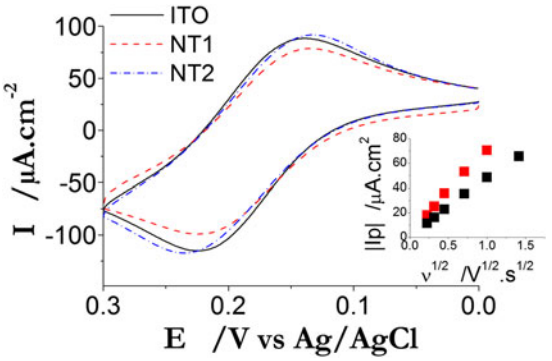


FIG. 6. Cyclic voltammograms of the $Fe(CN)_6^{3-}/Fe(CN)_6^{4-}$ couple measured with an ITO film, two (CoMoCAT) CNT films as working electrodes. "NT1" and "NT2" films had respective surface resistivities of 94 and 212 Ω/sq. The inset shows the linear evolution of the anodic $\left(I_p^a\right)$ peak currents as a function of $\nu^{1/2}$ for NT1 film (red dots) and ITO (black dots).

The effect of cathodic treatment in acidic conditions on the electroactivity was investigated by electrochemical impedance spectroscopy (EIS). Figure 7 shows the spectra measured at the CNT film, at 0.18 V, i.e., the standard potential of the $[Fe(CN)_6^{3-}/Fe(CN)_6^{4-}]$ redox couple. The electrodes were treated with 10 polarization cycles from 0.2 to −1.2 V at a scan rate of 0.1 V/s in acidic aqueous solutions. In the case of CNT films, the above treatment resulted in an improved electroactivity than in the pristine films. A significant decrease of the charge transfer resistance, from ~600 to <320 Ω cm^{-2}, is in fact observed after treatment at pH 5 and even larger at pH 3. Such a behavior may be attributed to the removal of defects, such as oxidized sp^3 groups onto the CNT surface, during the cathodic treatment that would improve its electrocatalytic performance. The effect of the surface state upon the charge transfer kinetics on CNT electrodes has been the subject of numerous investigations, which have shown that the electrochemical pretreatments are, in particular, able to change the electronic properties of the carbon material producing different electrocatalytic behaviors.[55] In addition, the pristine CNT films show values of the double layer capacitance typical for electrolytic aqueous solutions (15–20 µF cm^{-2}). Although the above treatment results in an increase of the charge transfer resistance, no significant difference was observed in the double layer capacitance.

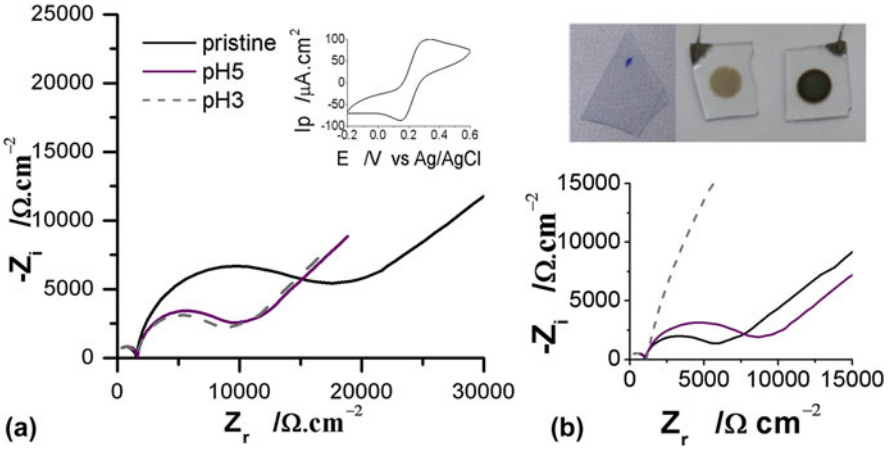


FIG. 7. (a) EIS of (CCNI) CNT film and (b) EIS of ITO glass. For both electrodes, EIS has been done before any treatment and after acidic treatment at pH 5 and pH 3, in 0.1 M KCl + 1 mM $Fe(CN)_6^{3-}/Fe(CN)_6^{4-}$ solution. A treatment is 10 cathodic polarization cycles from 0.2 to −1.2 V at 0.1 V/s. Pictures of ITO substrates from the left to the right: before treatment and after treatment at pH 5 and pH 3. ITO surface changes color when exposed to the treatment; the circle part is due to the electrochemical cell design. Inset to a: the cyclic voltammogram of the $Fe(CN)_6^{3-}/Fe(CN)_6^{4-}$ couple measured with the film used for EIS. This film had a surface resistivity of 189 Ω/sq.

https://doi.org/10.1557/jmr.2015.166 Published online by Cambridge University Press

This is a further indication that the cathodic treatment improved the kinetics of the electrochemical reaction maintaining unchanged the morphology of the electrode surface.

By contrast, in the case of the ITO electrode, the same treatment brought about a strong increase of the charge transfer resistance and of the capacitance of the double layer, both associated to the known instability of such material at negative potentials and under acidic condition that, after prolonged treatment, leads to its complete inactivity, as shown in Fig. 7(b).

V. CONCLUSIONS

Uniform and homogeneous TCFs have been made by filtration of different CNT solutions prepared either by the reductive dissolution route or by the aqueous dispersion technique. CNT length appears as a key parameter to control the electrical properties of the CNT TCFs. Avoiding sonication and high shear mixing, the reductive dissolution preserves the pristine nanotube length. It is thus a choice method to prepare TCFs and other devices/composites where CNT length is crucial. Of course, this is not the sole important factor. Defects induced by sonication, high shear mixing, covalent functionalization, or any other relatively aggressive method to disperse CNTs can further downgrade the properties of TCFs. This is why the reductive dissolution method used in this work outperforms by far the conventional sonication and surfactant assisted dispersion method, beyond the simple advantage of achievement of longer CNTs. Indeed, CNT defects and metallic/semiconductor CNT ratio add a synergetic effect that may explain the strong dependency of the TCF sheet resistance observed with the CNT length. Furthermore, the CNT films can profitably substitute ITO as electrode materials, especially in acidic conditions, where CNTs show a superior stability than ITO. The CNT films' electroactivity improves in fact at negative potentials, a possible doping effect from the acidic medium.

VI. EXPERIMENTAL

A. Materials

The CNTs used to make films are all produced by CVD. Elicarb CNTs from Thomas Swan are CNTs composed of one to three walls. They are called FWCNTs. MWCNTs were produced by Arkema. SWCNTs (CoMoCAT) were purchased from SWeNT. Different batches of SWCNTs have been used (CG200 and CG100). SWCNTs from CCNI have been used for electrochemical experiments. Sodium cholate purchased to Sigma–Aldrich is used as surfactant to prepare aqueous dispersions. DMSO is used as organic polar solvent to dissolve CNT salts in the process of reductive dissolution and was purchased from Sigma–Aldrich. This solvent was filtered over a 20 nm pore size membrane before use. THF is used to prepare the reductive solution and was purchased from Sigma–Aldrich. All organic solvents used during the reductive dissolution process are dried over alumina before use under inert atmosphere.

B. Aqueous dispersions and their subsequent films (ad-CNTs)

Aqueous dispersions of CNTs were prepared by ultrasonication with sodium cholate as surfactant. FWCNTs and MWCNTs dispersions were prepared at 0.3% wt of CNTs, and SWCNT dispersions were prepared with only 0.1% wt of CNTs. In all cases, the ratio CNT: surfactant is of 1:1 in weight. The concentration of sodium cholate is maintained near the critical micellar concentration to allow a good dispersion, but below a concentration where depletion phenomenon can occur to avoid further interactions between CNTs, as shown by Maillaud et al.[56] The SWCNT dispersion required a slight centrifugation (30 min at 1800 g) to remove the residual aggregates. A good dispersion of CNTs without any aggregates visible under optical microscope is obtained after an hour of sonication at a power of 25 W and centrifugation. Then CNT dispersions were filtered on cellulose membranes to obtain thin films. Finally, the films were transferred on different substrates, such as PET or glass substrates, using the method described previously by Martel et al.[1]

C. Solutions and films by solvent method (rd-CNTs)

The same CNTs were used to prepare true solutions as described previously[15] using the reductive dissolution method of CNTs in a polar solvent, such as DMSO. The first step consists in the reduction of CNTs by a solution of potassium naphthalenide in THF.[20] The stoichiometry of the salt is controlled at this step and kept at KC_{10}. After drying, 8 mg of salt is added to 1 mL of DMSO and stirred at room temperature overnight. A centrifugation (2500 g, 1 h) led to solutions with concentrations of 2 mg/mL of FWCNTs and 1.7 mg/mL of MWCNTs.

rd-CNT films were prepared by filtration on alumina membranes and then transferred on substrates.[29] The whole process has to be realized under inert atmosphere until the filtration is done. Only the transfer is performed in ambient air. It consists in the dissolution of the alumina membrane in a sodium hydroxide bath. While the membrane is removed, the film is floating on the liquid of the bath. After rinsing with distilled water to neutralize the bath, a substrate is immersed under the rd-CNT film, which is gently deposited on the substrate, by removing water. Finally, the film is dried at 50 °C overnight.

https://doi.org/10.1557/jmr.2015.166 Published online by Cambridge University Press

D. DLS measurements

Average length of CNTs was measured by DLS. The experiments were performed at 20 °C using a continuous diode laser Excelsior Spectra-Physics at a wave length of 644 nm with a maximum power $P = 100$ mW and a Brookhaven BI-90000AT digital autocorrelator (Holtsville, NY) to compute the scattered intensity time autocorrelation function. A routine method was developed by Badaire et al.[36] to calculate the length of CNTs based on Broersma's relations for rigid rods.[57,58]

E. Scanning electron microscopy (SEM)

SEM observations were performed with a JEOL 6700F scanning electron microscope (JEOL, Tokyo, Japan) operating at 5 kV. Samples were coated with a nm-thick layer of gold palladium (10%) with a SC7620 Sputter coater (Quorum Technologies, Laughton, East Sussex, UK) or JFC1200 Fine coater (JEOL, Tokyo, Japan) before analysis.

F. Electrical measurements

Surface resistivity of FWCNT and MWCNT films has been measured using a two contact method. Surface resistivity of SWCNT films has been measured using a four contact method. For this characterization, four gold electrodes are sputtered through a mask over CNT films. Geometry of the electrodes is well controlled to allow a good comparison of the surface resistivity of CNT films.

G. Electrochemistry

Electrochemical experiments were performed with a three electrode cell controlled by a 650D electrochemical workstation from CH Instrument, Inc. using an Ag/AgCl electrode and a platinum wire as respectively reference electrode and counter electrode. Working electrode was either CNT films or ITO glass depending on the experiments.

A cathodic polarization was performed from 0.2 to −1.2 V at pH 5 and pH 3 in buffered solutions to treat CNT films and ITO glass. CV and EIS were carried out in aqueous solution containing KCl at 0.1 M as supporting electrolyte and a redox couple $Fe(CN)_6^{3-}/Fe(CN)_6^{4-}$ at 1 mM, before and after each treatment to control the effect of the treatment. The EIS was performed from 0.1 to 10^6 Hz, at 180 mV corresponding to the half-wave potential of the redox couple.

ACKNOWLEDGMENTS

AC thanks Arkema and l'Association Nationale pour la Recherche et la Technologie (ANRT) for a PhD grant. Support from the Agence Nationale de la Recherche (IMPEC Project) is acknowledged. AP thanks Dr H. Saadaoui for the inset of Fig. 1(a) and the Aquitaine region for a grant to support collaboration with the Emilia Romagna region. This work has been performed within the framework of the GDR-I 3217 "graphene and nanotubes".

REFERENCES

1. C.M. Aguirre, S. Auvray, S. Pigeon, R. Izquierdo, P. Desjardins, and R. Martel: Carbon nanotube sheets as electrodes in organic light-emitting diodes. *Appl. Phys. Lett.* **88**, 183104 (2006).
2. E. Artukovic, M. Kaempgen, D.S. Hecht, S. Roth, and G. Grüner: Transparent and flexible carbon nanotube transistors. *Nano Lett.* **5**, 757–760 (2005).
3. Z. Wu, Z. Chen, X. Du, J.M. Logan, J. Sippel, M. Nikolou, K. Kamaras, J.R. Reynolds, D.B. Tanner, A.F. Hebard, and A. Rinzler: Transparent, conductive carbon nanotube films. *Science* **305**, 1273–1276 (2004).
4. R. Andrews, D. Jacques, M. Minot, and T. Rantell: Fabrication of carbon multiwall nanotube/polymer composites by shear mixing. *Macromol. Mater. Eng.* **287**, 395–403 (2002).
5. B. Vigolo, A. Penicaud, C. Coulon, C. Sauder, R. Pailler, C. Journet, P. Bernier, and P. Poulin: Macroscopic fibers and ribbons of oriented carbon nanotubes. *Science* **290**, 1331–1334 (2000).
6. L. Viry, C. Mercader, P. Miaudet, C. Zakri, A. Derré, A. Kuhn, M. Maugey, and P. Poulin: Nanotube fibers for electromechanical and shape memory actuators. *J. Mater. Chem.* **220**, 3487–3495 (2010).
7. T. Fukushima, K. Asaka, A. Kosaka, and T. Aida: Fully plastic actuator through layer-by-layer casting with ionic-liquid-based bucky gel. *Angew. Chem. Int. Ed. Engl.* **44**, 2410–2413 (2005).
8. C. Bartholome, A. Derré, O. Roubeau, C. Zakri, and P. Poulin: Electromechanical properties of nanotube–PVA composite actuator bimorphs. *Nanotechnology* **19**, 325501 (2008).
9. G.B. Blanchet, C.R. Fincher, and F. Gao: Polyaniline nanotube composites: A high-resolution printable conductor. *Appl. Phys. Lett.* **82**, 1290–1292 (2003).
10. K. Saint-Aubin, P. Poulin, H. Saadaoui, M. Maugey, and C. Zakri: Dispersion and film-forming properties of poly(acrylic acid)-stabilized carbon nanotubes. *Langmuir* **25**, 13206–13211 (2009).
11. K. Shen, S. Curran, H. Xu, S. Rogelj, Y. Jiang, J. Dewald, and T. Pietrass: Single-walled carbon nanotube purification, pelletization, and surfactant-assisted dispersion: A combined TEM and resonant micro-raman spectroscopy study. *J. Phys. Chem. B* **10**, 4455–4463 (2005).
12. K.L. Lu, R.M. Lagon, Y.K. Chen, M.L.H. Green, and P.J.F. Harris: Mechanical damage of carbon nanotubes by ultrasound. *Carbon* **34**, 814–816 (1996).
13. A. Lucas, C. Zakri, M. Maugey, M. Pasquali, P. vd Schoot, and P. Poulin: Kinetics of nanotube and microfiber scission under sonication. *J. Phys. Chem. C* **113**, 20599–20605 (2009).
14. G. Pagani, M.J. Green, P. Poulin, and M. Pasquali: Competing mechanisms and scaling laws for carbon nanotube scission by ultrasonication. *Proc. Natl. Acad. Sci. U. S. A.* **109**, 11599–11604 (2012).
15. A. Pénicaud, P. Poulin, A. Derré, E. Anglaret, and P. Petit: Spontaneous dissolution of a single-wall carbon nanotube salt. *J. Am. Chem. Soc.* **127**, 8–9 (2005).
16. S. Fogden, C. Howard, R.K. Heenan, N.T. Skipper, and M.S.P. Shaffer: Scalable method for the reductive dissolution, purification, and separation of single-walled carbon nanotubes. *ACS Nano* **6**, 54–62 (2012).
17. S. Fogden, K. Kim, C. Ma, and G. McFarlane: Scalable single walled carbon nanotube separation: From process to product. *NSTI-Nanotech*, Boston, MA, 2011; pp. 163–166.

https://doi.org/10.1557/jmr.2015.166 Published online by Cambridge University Press

18. C. Jiang, A. Saha, C. Xiang, C.C. Young, J.M. Tour, M. Pasquali, and A.A. Marti: Increased solubility, liquid-crystalline phase, and selective functionalization of single-walled carbon nanotube polyelectrolyte dispersions. *ACS Nano* **7**, 4503–4510 (2013).
19. B. Vigolo, C. Hérold, J-F. Marêché, P. Bourson, S. Margueron, J. Ghanbaja, and E. McRae: Direct revealing of the occupation sites of heavy alkali metal atoms in single-walled carbon nanotube intercalation compounds. *J. Phys. Chem. C* **113**, 7624–7628 (2009).
20. P. Petit, C. Mathis, C. Journet, and P. Bernier: Tuning and monitoring the electronic structure of carbon nanotubes. *Chem. Phys. Lett.* **305**, 370–374 (1999).
21. D. Voiry, C. Drummond, and A. Penicaud: Portrait of carbon nanotube salts as soluble polyelectrolytes. *Soft Matter* **7**, 7998 (2011).
22. A. Pénicaud, F. Dragin, G. Pécastaings, M. He, and E. Anglaret: Concentrated solutions of individualized single walled carbon nanotubes. *Carbon* **67**, 360–367 (2014).
23. M. Senthilkumar, J. Mathiyarasu, J. Joseph, K.L.N. Phani, and V. Yegnaraman: Electrochemical instability of indium tin oxide (ITO) glass in acidic pH range during cathodic polarization. *Mater. Chem. Phys.* **108**, 403–407 (2008).
24. K.E. Lee, M. Wang, E.J. Kim, and S.H. Hahn: Structural, electrical and optical properties of sol–gel AZO thin films. *Curr. Appl. Phys.* **9**, 683–687 (2009).
25. S. Bae, H. Kim, Y. Lee, X. Xu, J.S. Park, Y. Zheng, J. Balakrishnan, T. Lei, H.R. Kim, Y.I. Sng, Y-J. Kim, K.S. Kim, B. Özyilmaz, J-H. Ahn, B.H. Hong, and S. Iijima: Roll-to-roll production of 30-inch graphene films for transparent electrodes. *Nat. Nanotechnol.* **5**, 574–578 (2010).
26. M.G. Kang, M.S. Kim, J. Kim, and L.J. Guo: Organic solar cells using nanoimprinted transparent metal electrodes. *Adv. Mater.* **20**, 4408–4413 (2008).
27. D.S. Hecht, L. Hu, and G. Irvin: Emerging transparent electrodes based on thin films of carbon nanotubes, graphene, and metallic nanostructures. *Adv. Mater.* **23**, 1482–1513 (2011).
28. A. Kumar and C. Zhou: The race to replace tin-doped indium oxide: Which material will win? *ACS Nano* **4**, 11–14 (2010).
29. T. Minami and T. Miyata: Present status and future prospects for development of non- or reduced-indium transparent conducting oxide thin films. *Thin Solid Films* **517**, 1474–1477 (2008).
30. Y. Zhou, L. Hu, and G. Grüner: A method of printing carbon nanotube thin films. *Appl. Phys. Lett.* **88**, 12 (2006).
31. B. Dan, G.C. Irvin, and M. Pasquali: Continuous and scalable fabrication of transparent conducting carbon nanotube films. *ACS Nano* **3**, 835–843 (2009).
32. M.D. Lima, M.J. de Andrade, C.P. Bergmann, and S. Roth: Thin, conductive, carbon nanotube networks over transparent substrates by electrophoretic deposition. *J. Mater. Chem.* **18**, 776–779 (2008).
33. Y.I. Song, C.M. Yang, D.Y. Kim, H. Kanoh, and K. Kaneko: Flexible transparent conducting single-wall carbon nanotube film with network bridging method. *J. Colloid Interface Sci.* **318**, 365–371 (2008).
34. C.L. Pint, Y.Q. Xu, M. Pasquali, and R.H. Hauge: Formation of highly dense aligned ribbons and transparent films of single-walled carbon nanotubes directly from carpets. *ACS Nano* **2**, 1871–1878 (2008).
35. F. Mirri, A.W.K. Ma, T.T. Hsu, N. Behabtu, S.L. Eichmann, C.C. Young, D.E. Tsentalovich, and M. Pasquali: High-performance carbon nanotube transparent conductive films by scalable dip coating. *ACS Nano* **6**, 9737–9744 (2012).
36. S. Badaire, P. Poulin, M. Maugey, and C. Zakri: In situ measurements of nanotube dimensions in suspensions by depolarized dynamic light scattering. *Langmuir* **20**, 10367–10370 (2004).
37. A.M. Shetty, G.M.H. Wilkins, J. Nanda, and M.J. Solomon: Multiangle depolarized dynamic light scattering of short functionalized single-walled carbon nanotubes. *J. Phys. Chem. C* **113**, 7129 (2009).
38. A. Pénicaud, P. Petit, and J.E. Fischer: Doped carbon nanotubes. In *Carbon Meta-Nanotubes: Synthesis, Properties and Applications*, M. Monthioux ed. (John Wiley & Sons, Hoboken, NJ, 2012); pp. 41, 111.
39. F. Khoerunnisa, A. Morelos-Gomez, H. Tanaka, T. Fujimori, D. Minami, R. Kukobat, T. Hayashi, S.Y. Hong, Y.C. Choi, M. Miyahara, M. Terrones, M. Endo, and K. Kaneko: Metal–semiconductor transition like behavior of naphthalene-doped single wall carbon nanotube bundles. *Faraday Discuss.* **173**, 145–156 (2014).
40. C. Li, E.T. Thostenson, and T-W. Chou: Dominant role of tunneling resistance in the electrical conductivity of carbon nanotube-based composites. *Appl. Phys. Lett.* **91**, 223114 (2007).
41. Y. Ma, W. Cheung, D. Wei, A. Bogozi, P.L. Chiu, L. Wang, F. Pontoriero, R. Mendelsohn, and H. He: Improved conductivity of carbon nanotube networks by in situ polymerization of a thin skin of conducting polymer. *ACS Nano* **2**, 1197–1204 (2008).
42. S.B. Yang, B-S. Kong, D-H. Jung, Y-K. Baek, C-S. Han, S-K. Oh, and H-T. Jung: Recent advances in hybrids of carbon nanotube network films and nanomaterials for their potential applications as transparent conducting films. *Nanoscale* **3**, 1361–1373 (2011).
43. D. Hecht, L. Hu, and G. Grüner: Conductivity scaling with bundle length and diameter in single walled carbon nanotube networks. *Appl. Phys. Lett.* **89**, 133112 (2006).
44. D.T.N. Chen, K. Chen, L.A. Hough, M.F. Islam, and A.G. Yodh: Rheology of carbon nanotube networks during gelation. *Macromolecules* **43**, 2048 (2010).
45. D. Simien, J.A. Fagan, W. Luo, J.F. Douglas, K. Migler, and J. Obrzut: Influence of nanotube length on the optical and conductivity properties of thin single-wall carbon nanotube networks. *ACS Nano* **2**, 1879 (2008).
46. R.M. Snider, M. Ciobanu, A.E. Rue, and D.E. Cliffel: A multiwalled carbon nanotube/dihydropyran composite film electrode for insulin detection in a microphysiometer chamber. *Anal. Chim. Acta.* **609**, 44–52 (2008).
47. L.H. Nguyen, T.V. Phi, P.Q. Phan, H.N. Vu, C. Nguyen Duc, and F. Fossard: Synthesis of multi-walled carbon nanotubes for NH_3 gas detection. *Phys. E* **37**, 54–57 (2007).
48. H. Xu, Q. Zheng, P. Yang, J. Liu, and L. Jin: Sensitive voltammetric detection of trace heavy metals in real water using multi-wall carbon nanotubes/nafion composite film electrode. *Chin. J. Chem.* **29**, 805–812 (2011).
49. M. Grätzel: Photoelectrochemical cells. *Nature* **414**, 338–344 (2001).
50. J.E. Trancik, S.C. Barton, and J. Hone: Transparent and catalytic carbon nanotube films. *Nano Lett.* **8**, 982–987 (2008).
51. D. Noureldine, T. Shoker, M. Musameh, and T.H. Ghaddar: Investigation of carbon nanotube webs as counter electrodes in a new organic electrolyte based dye sensitized solar cell. *J. Mater. Chem.* **22**, 862–869 (2012).
52. L. Kavan: Exploiting nanocarbons in dye-sensitized solar cells. *Top. Curr. Chem.* **348**, 53–93. In *Making and Exploiting Fullerenes, Graphene, and Carbon Nanotubes*, M. Marcaccio and F. Paolucci eds. (Springer, Berlin Heidelberg, Germany, 2014).
53. M.J. Alam and D.C. Cameron: Optical and electrical properties of transparent conductive ITO thin films deposited by sol-gel process. *Thin Solid Films* **377–378**, 455–459 (2000).

https://doi.org/10.1557/jmr.2015.166 Published online by Cambridge University Press

54. J. Stotter, Y. Show, S. Wang, and G. Swain: Comparison of the electrical, optical, and electrochemical properties of diamond and indium tin oxide thin-film electrodes. *Chem. Mater.* **17**, 4880–4888 (2005).
55. F. Valentini, A. Amine, S. Orlanducci, M.L. Terranova, and G. Palleschi: Carbon nanotube purification: Preparation and characterization of carbon nanotube paste electrodes. *Anal. Chem.* **75**, 5413–5421 (2003).
56. L. Maillaud, C. Zakri, I. Ly, A. Pénicaud, and P. Poulin: Conductivity of transparent electrodes made from interacting nanotubes. *Appl. Phys. Lett.* **103**, 263106 (2013).
57. S. Broersma: Rotational diffusion constant of a cylindrical particle. *J. Chem. Phys.* **32**, 1626 (1960).
58. S. Broersma: Viscous force and torque constants for a cylinder. *J. Chem. Phys.* **74**, 6989 (1981).

https://doi.org/10.1557/jmr.2015.166 Published online by Cambridge University Press